# Approaches for Efficient Modeling of the Mechanical Response of Complex Periodic Truss Architectures

Carlos M. Portela[1], Gregory P. Phlipot[1] , Julia R. Greer[1], and Dennis M. Kochmann[2]

[1]California Institute of Technology
Pasadena, California

[2]ETH Zürich
Zürich, Switzerland

## ABSTRACT

With recent advances in additive manufacturing techniques, the ability to design the microstructure of macroscopic geometries have opened up the ability to create a new class of tunable metamaterials, including periodic truss lattices. While the experimentalists have the ability to manufacture and test truss lattices with various constituent materials, topologies, and relative densities undergoing various loading cases, the ability to predict the mechanical response of these lattices through simulation remains a challenge due in part to the non-slender nature of the manufacturable lattices. Further challenges are introduced by the computational expense associated with modeling these multiscale metamaterials, which might involve the simulation of millions of structural components. In this paper, we first explore how the properties of non-slender truss lattices differ from the slender lattice theory by performing experiments on moderate relative density truss lattices with changes in node geometry. Then we address both of the computational challenges by developing reduced order models of non-slender truss lattices and a computational framework built on the quasicontinuum (QC) method to reduce the computational cost of modeling periodic slender truss lattices consisting of a large number of truss members. We then outline how the reduced order models can be combined in the QC framework to model large non-slender lattices.

## 1. INTRODUCTION

The microstructure of periodic truss lattices can be designed in order to obtain certain desirable macroscopic properties of the effective metamaterial, including high stiffness- and strength-to-weight ratios, tunable acoustic properties, and energy absorption [1–3]. A significant amount of work has been done by using beam theory and homogenization techniques to catalog the macroscopic properties that arise from various periodic truss lattices [4–6]. However, the use of beam and homogenization theory means that the analysis is only valid for slender lattices with a separation of scales between the size of the unit cell to the smallest macroscopic length scale. Most truss lattices currently being manufactured consist of non-slender beams, and many interesting applications of the lattices involve situations where a separation of scales does not exist (e.g., fracture).

*Copyright 2019. Used by the Society of the Advancement of Material and Process Engineering with permission.*

*SAMPE Conference Proceedings. Charlotte, NC, May 20-23, 2019. Society for the Advancement of Material and Process Engineering – North America.*

Predicting the response of finite, non-slender truss lattices is challenging. Some authors resort to using continuum-level finite element models of the entire truss, but this results in extremely computationally intensive simulations which severely limits the size of the truss that can be simulated [1]. In this paper, we address this issue by outlining computational techniques that can be used to drastically reduce the computational cost of modeling large non-slender truss lattices without assuming a separation of scales.

First, the higher-order effects arising from the non-slender nature of truss lattices is investigated through experiments – showing the deviation from the predictions resulting from beam theory. Then, we use reduced order modeling techniques to drastically reduce the number of degrees of freedom (dofs) required to model the non-slender trusses, while still maintaining a high degree of accuracy. Subsequently, we outline a coarse-graining technique that can be used to model general periodic truss lattices – and demonstrate its effectiveness in reducing the cost of large nonlinear periodic truss simulations.

# 2. METHODS

## 2.1 Experiments on non-slender lattice architectures

Using advanced additive manufacturing techniques, several works have explored a wide range of geometric lattice parameters and their effects on the mechanical response of lattice materials. Using nano- to microscale techniques such as two-photon lithography and stereolithography, it has been shown that the effective material stiffness and strength fail to be predicted by classical scaling theories [1,3,7,8]. Such scaling theories [9] fall short since they rely on the applicability of beam theory, which becomes inaccurate for the vast majority of load-bearing applications due to the non-slender geometries, i.e., with large strut radius-to-length ratios $r/l$, required for those lattice materials. The deviation from the classical scaling laws has been attributed mostly to the effect of *nodes* or strut junctions, which become a larger fraction of the material as the relative density increases [10].

To explore this effect of nodes on lattice architectures for which beam theory is inaccurate, we fabricated microscale and centimeter-scale lattice architectures with varying node geometries and explored their effect on the stiffness response. The microscale samples were fabricated out of Ip-Dip polymer using a two-photon lithography (TPL) process (Nanoscribe GmbH), and had overall dimensions of 125×125×125 μm in a 5×5×5 unit cell tessellation. The self-similar centimeter-scale samples were fabricated out of PR-48 resin using a digital light processing (DLP) 3D printer (Autodesk). Since the mechanical response of lattices depends not only on the relative density and slenderness ratio (for a given material of choice), but also on the structural rigidity [11] of the unit cell, we fabricated samples of rigid *octahedron* and non-rigid *tetrakaidekahedron* geometries.

For each of the geometries, the nodes were modified by varying the cross-section throughout the struts such that a characteristic second area moment of the nodes, $I$, changed but the strut volume remained constant. In particular, the cross-section of the struts at nodes was changed from a circle

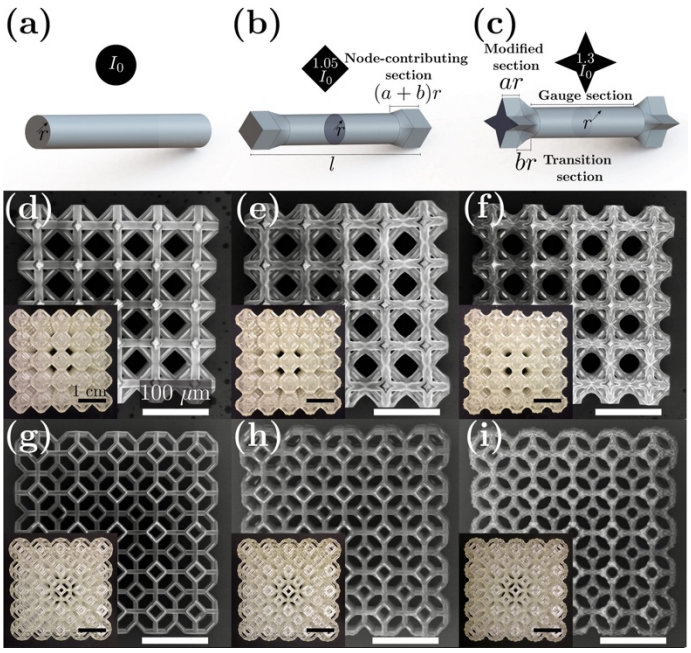



**Figure 1.** Modified-node experiments. (a) strut for circle cross section at node, (b) square cross section, and (c) star cross-section; (d)-(f) octahedron samples with circle, square, and star nodes, respectively; (g)-(i) tetrakaidekahedron samples with circle, square, and star nodes, respectively. The self-similar centimeter-scale samples are shown as insets. For this study, the variables *a* and *b* were chosen to be 1.5 and 1, respectively.

($I_0$), to a square ($1.05I_0$), and a star ($1.3I_0$) (Fig. 1). The slenderness ratio was also varied between $r/l = 0.07$, 0.10-0.11, and 0.15 for each combination of lattice and node geometry. The stiffness of each lattice architecture was probed at the microscale via nanomechanical compression experiments (Agilent G200), and at the macroscale using a load frame (Instron 5500). All compressions were done quasistatically to a strain of $\varepsilon = 0.35$ at a strain rate of $10^{-3}$ $s^{-1}$.

## 2.2 Modeling the linear response of non-slender lattice architectures

Since the stiffness response of lattices beyond slenderness ratios of $r/l \approx 0.07$ significantly deviates from the classical predictions [10], a numerical model consisting of solely beam elements would fail to predict the experimental response. On the other hand, a continuum finite element model would have to be restricted to a single unit cell with periodic boundary conditions (due to computational cost), and would fail to capture the finite nature of the samples and the subsequent effect of free boundaries.

To overcome these issues, we implemented a reduced-order model with full-detail resolution at nodes while the connecting struts were modeled as Timoshenko beam elements (Fig. 2). To further reduce computational cost, a static condensation of degrees of freedom was performed on the tetrahedron-meshed nodes such that only six degrees of freedom (three displacements and three rotations) were retained at each face where a beam was attached. This allowed each node to be treated as a single element with 6*z* dofs, with *z* struts connected to it, as opposed to a discretization of $\sim 10^3$ tetrahedral elements [12]. The strut dofs were then coupled in an on-average sense to the 6 dofs corresponding to each connecting face, which allowed for a full

$n \times n \times n$ tessellation to be modeled efficiently. For the architectures modeled in this study, the problem size (i.e., number of dofs) was reduced to 0.02-0.3 % of the original size. Even with this reduction in problem size, comparing the response of a reduced-order unit cell to that of a fully meshed unit cell resulted in a maximum error of 3%.

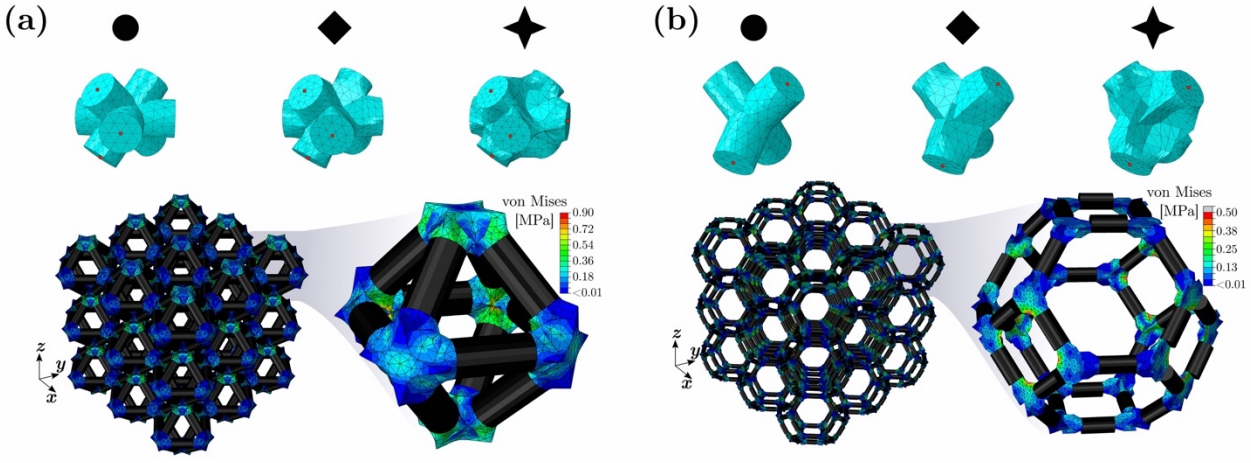



**Figure 2.** Reduced-order models. Representative circle, square, and star nodes for a representative $r/l = 0.07$ unit cell; representative 3×3×3 tessellation and detailed view of the stress distribution at the nodes for: (a) octahedron geometry, (b) tetrakaidekahedron geometry. The elements in black correspond to Timoshenko beam elements (10 elements per strut).

## 2.3 Reducing computational cost of large periodic truss lattice simulations

Due to their multiscale nature, periodic truss lattices can contain several million truss members. If the microstructure is resolved exactly everywhere (even using beams and reduced order models described above), modeling large truss lattices can be computationally expensive. Recently the quasicontinuum (QC) method – a set of kinematic constraints and energy approximation techniques used to drastically reduce the cost of atomic lattice simulations – has been extended to model simple 2D slender trusses undergoing small deformations and failure [13–16]. However, the QC method so far has only been used to model planar lattices than can be described by a single Bravais lattice (e.g. square, triangle, or cross-braced lattices). It has not been used to model 3D lattices, which are much more common, and the existing formulation cannot be used to model multilattice - more complex lattices that cannot be described by a single Bravais lattice (e.g. hexagon, kagome, tetrakaidecahedron). Here, we outline a formulation of the QC method for slender trusses (i.e. ignoring nodal effects) that can be used to model the *geometrically nonlinear* response of *2- and 3-dimensional multilattices* with an *adaptive refinement* technique to increase model resolution where necessary.

### 2.3.1 Fully-resolved problem

The formulation of the QC technique begins by looking at the expensive fully-resolved simulation where every truss member is modeled with a (possibly nonlinear) structural finite element. We investigate truss lattices that consist of an arrangement of unit cells $\Omega_u$ tessellated

along directions $\mathcal{B} = \{\boldsymbol{a_1}, \dots, \boldsymbol{a_d}\}$ in $d$ dimensions. The unit cells contain nodes, each with degrees of freedom $\boldsymbol{\varphi} = \{\boldsymbol{x}, \boldsymbol{\theta}\}$ representing the translational and rotational dofs of the node. We denote the dofs of all of the nodes in the unit cell as $\tilde{\boldsymbol{\varphi}} = \{\boldsymbol{\varphi_1}, \dots, \boldsymbol{\varphi_{n_b}}\}$ where $n_b$ is equivalent to the number of Bravais lattices used to describe the multilattice. The lattice also contains truss members. We denote the set of truss members that connect nodes inside the same unit cell as $\mathcal{E}_u$, while the truss members connected to nodes in neighboring unit cells are given by the set $\mathcal{E}_u^{\mathcal{N}}$ (Fig. 3). Assuming a general form for the energy of a truss member $W_e(\boldsymbol{\varphi_1}, \boldsymbol{\varphi_2})$ where $\boldsymbol{\varphi_1}, \boldsymbol{\varphi_2}$ are the dofs of the nodes of the truss member, the total potential energy of the lattice can be expressed as a sum over unit cell energies

$$\begin{aligned} \mathcal{I}(\tilde{\boldsymbol{\varphi}}) &= \sum_{\Omega_u} W_u\left(\tilde{\boldsymbol{\varphi}}_{\boldsymbol{u}}, \tilde{\boldsymbol{\varphi}}_{\boldsymbol{\mathcal{N}(u)}}\right) - \mathcal{L}, \\ W_u\left(\tilde{\boldsymbol{\varphi}}_{\boldsymbol{u}}, \tilde{\boldsymbol{\varphi}}_{\boldsymbol{\mathcal{N}(u)}}\right) &= \sum_{e \in \mathcal{E}_u} W_e(\boldsymbol{\varphi_1}, \boldsymbol{\varphi_2}) - \frac{1}{2} \sum_{e \in \mathcal{E}_u^{\mathcal{N}}} W_e(\boldsymbol{\varphi_1}, \boldsymbol{\varphi_2}) \end{aligned} \tag{1}$$

where $\mathcal{L}$ is the prescribed external force potential. The boundary value problem can then be expressed as minimizing $\mathcal{I}$ over all dofs that satisfy desired essential boundary conditions.

This fully-resolved problem is expensive for two reasons: 1) The set of admissible dofs that satisfy the essential boundary conditions is very large – resulting in a large linear system to be solved in each Newton iteration, and 2) the computation of the energetic quantities (energy, force, stiffness matrix) require a sum over all of the unit cells in the periodic truss lattice, which is expensive. Therefore, the QC addresses the two issues by using kinematic constraints to reduce the size of the problem, and energy approximation techniques to inexpensively approximate the energy.

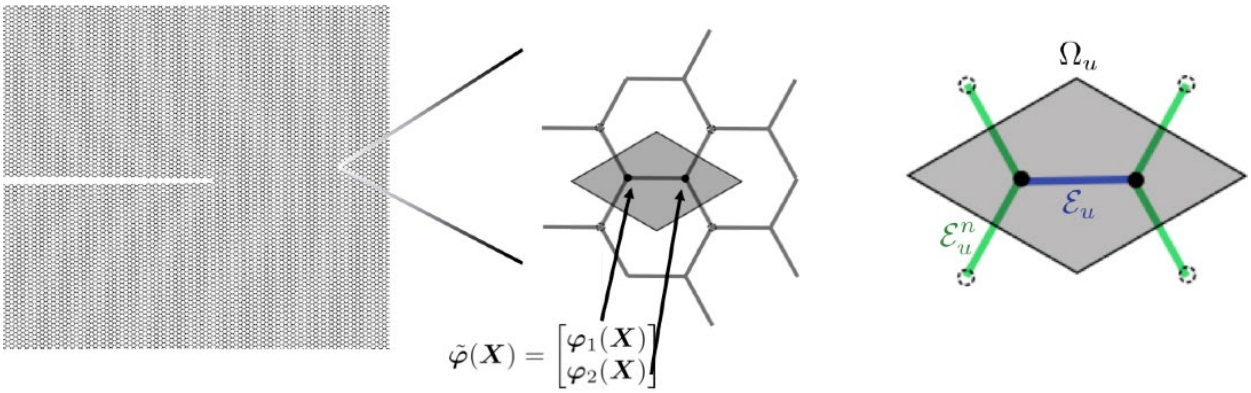



**Figure 3.** An example of the fully resolved problem showing an example geometry (left) made up of a tessellation of unit cells. The dofs of the unit cell (center) and the sets representing the truss members (right).

2.3.2 Kinematic constraints

The kinematic constraints are created by first selecting a subset of unit cells $N_{rep} \ll N$ called repUCs, that retain all of the dofs of all of the nodes in the unit cell, while the dofs of the remaining unit cells are constrained to be interpolated from the dofs of the repUCs,

$$\tilde{\boldsymbol{\varphi}}^h = \sum_{i=1}^{N_{rep}} N_i(\boldsymbol{X})\tilde{\boldsymbol{\varphi}}_{\boldsymbol{i}}(\boldsymbol{X}) \tag{2}$$

where $N_i(\boldsymbol{X})$ and $\boldsymbol{\varphi}_i(\boldsymbol{X})$ are the interpolation functions and dofs of the $i^{th}$ repUC resulting in the constrained dofs $\tilde{\boldsymbol{\varphi}}^h$. Here, we use linear finite element shape functions on a Delaunay triangulated mesh (Fig. 4), with the nodes of the mesh are the repUCs.

2.3.3 Energy approximation

In the QC literature, there are numerous energy approximation techniques known as summation or sampling rules. The most common sampling rules attempt to approximate the energy as a weighted sum over $N_s \ll N$ sampling unit cells such that

$$\mathcal{I}(\tilde{\boldsymbol{\varphi}}^{\boldsymbol{h}}) \approx \mathcal{I}^h(\tilde{\boldsymbol{\varphi}}^{\boldsymbol{h}}) = \sum_{i=1}^{N_s} w_s\, W_u\left(\tilde{\boldsymbol{\varphi}}^{\boldsymbol{h}}{}_{\boldsymbol{u}}, \tilde{\boldsymbol{\varphi}}^{\boldsymbol{h}}{}_{\boldsymbol{\mathcal{N}(u)}}\right)., \tag{3}$$

where $w_s$ are the sampling weights associated with each sampling unit cell. Here, we use the optimal summation rule, which consists of placing a sampling unit cell at each repUC location with a sample weight of one, and a Cauchy Born sampling unit cell at the centroid of each coarse-grained element with a weight that represents the number of unit cells inside the coarse element (see [17,18] for details). It is worth noting that in regions where every unit cell is a repUC, the weight of the Cauchy Born sampling unit cell is zero, therefore the exact kinematics and energy are naturally computed. Figure 4 gives an example of a QC mesh with the repUC and sampling unit cell locations in the optimal summation rule labeled.

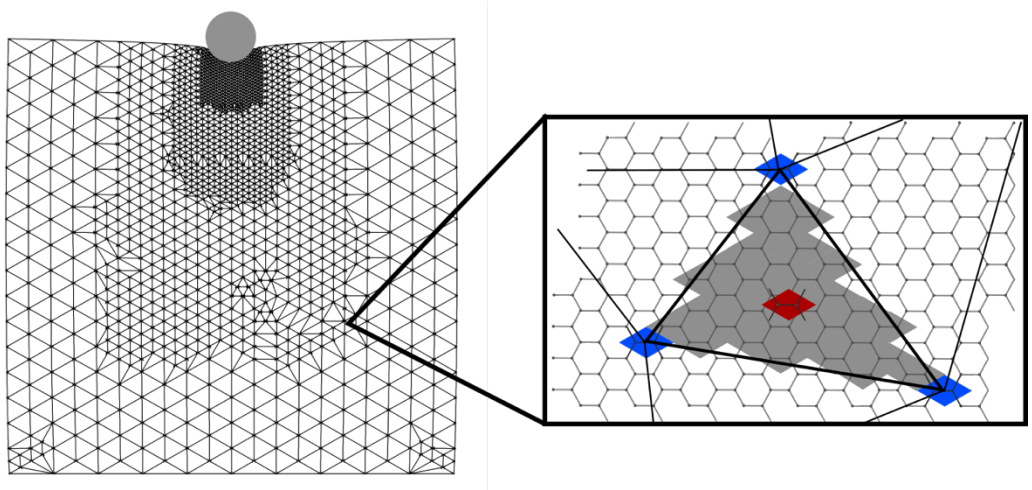


**Figure 4**. Example QC mesh (left), and a zoom in of a typical coarse-grained element (right). The blue unit cells are the repUCs and sample unit cells with weight 1, the red unit cell is the Cauchy Born unit cell, and the gray unit cells have their dofs interpolated from the repUCs.

# 3. RESULTS

## 3.1 Reduced-order model predicted stiffnesses

The reduced-order computational models showed that structural rigidity significantly affects the distribution of strain energy between struts and nodes. In particular, the rigid octahedron models show a transition from a strut-dominated distribution to a node-dominated distribution as $r/l$ increased. In comparison, the non-rigid tetrakaidekahedron architecture remains node-dominant throughout with a further increase in strain energy at nodes as $r/l$ increased (Fig. 5a,b). This ratifies the importance of capturing the physics at nodes for non-slender lattice architectures.

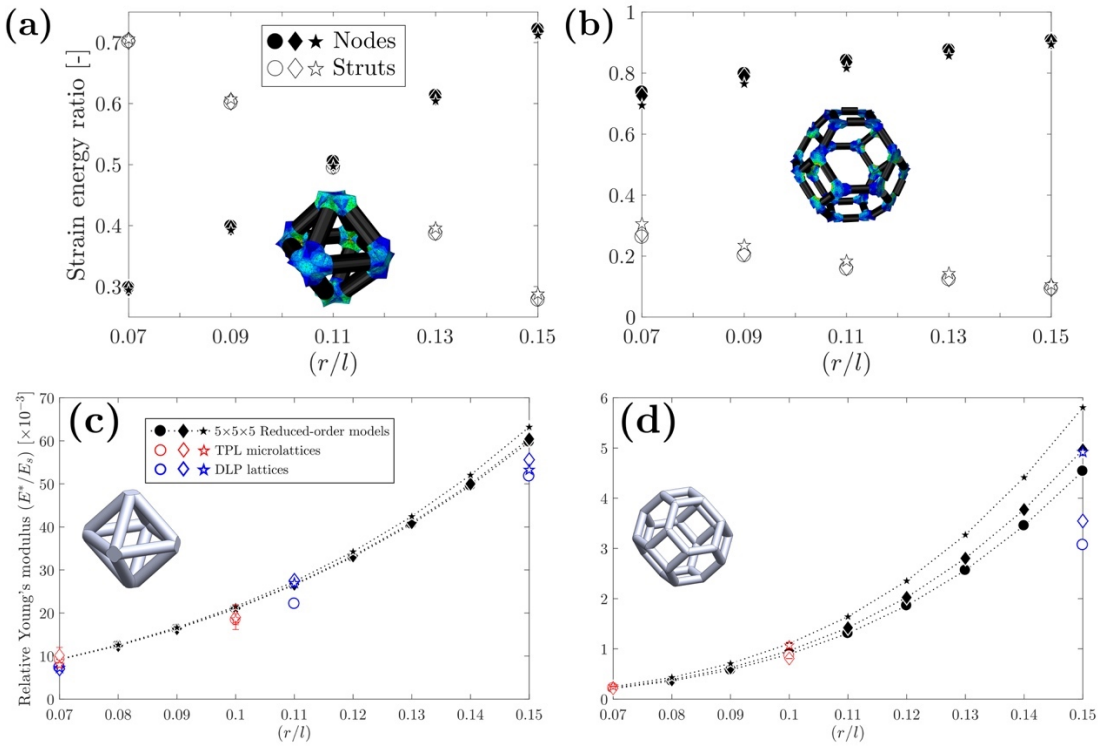



**Figure 5.** Strain energy distribution between nodes and struts in reduced-order models for (a) octahedron geometry, (b) tetrakaidekahedron geometry. Comparison of micro- and centimeter-scale experiments to reduced-order models for (a) octahedron geometry, (b) tetrakaidekahedron geometry.

Comparing the results of the experiments at the two scales to the reduced-order models shows exceptional agreement throughout the probed $r/l$ regime. Additionally, a more significant effect of node geometry on stiffness was observed for the tetrakaidekahedron than for the octahedron, as expected from a greater distribution of strain energy at its nodes.

## 3.2 Spherical indentation of 3D lattice using the QC method

In order to showcase the computational advantages of using the QC method outlined in section 2.3, we simulate a 10% relative density 3D kagome lattice (multilattice) undergoing spherical

indentation using both the fully-resolved approach (where every beam is modeled by a beam finite element) and the QC approach. The truss lattice specimen fills a box with side length $35l$ where $l$ is the length of a beam of the lattice. The spherical indenter has a radius $r = 5l$, and indents into the specimen a distance of $6l$. Geometric nonlinearity is incorporated into the model by using a corotational beam energy to describe each truss member. The use of corotational beams (see [18] for details on the formulation) enables to model to capture buckling of the truss lattice underneath the indenter. The QC simulation has a small fully-resolved region directly under the indenter, and is gradually coarsened away in the rest of the domain, using only 3.5% of the unit cells as repUCs (Fig. 6). We use an adaptive refinement technique (also outlined in [18]) to add new repUCs in highly deformed areas on-the-fly during the simulation.

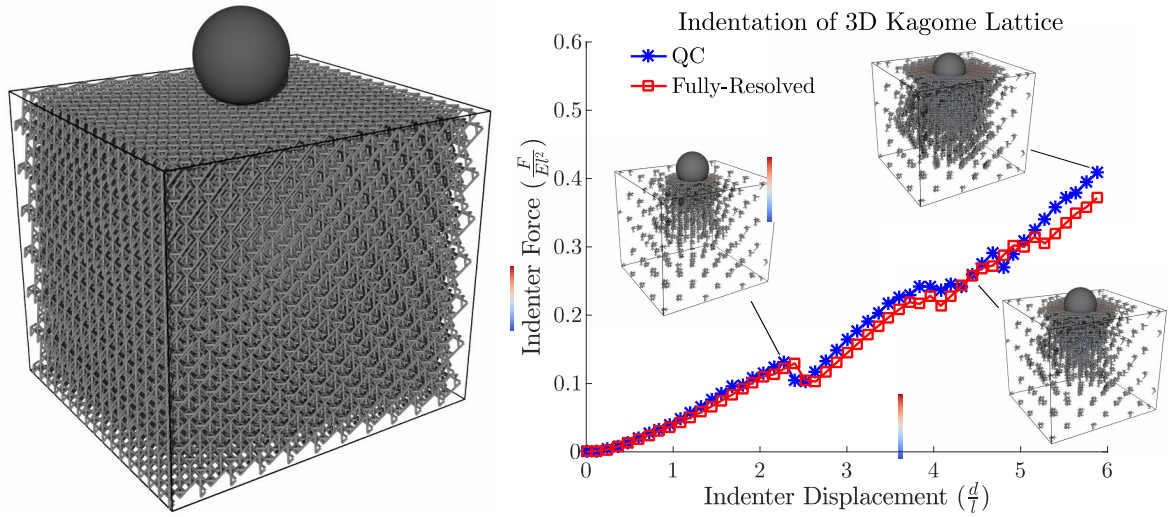



**Figure 6**. Undeformed geometry of the fully resolved simulation (left) and comparison of the normalized force-displacement of the indenter in the QC and fully-resolved simulations. The insets show all of the repUCs in the QC simulation as the mesh is adaptively refined throughout the simulation.

# 4. DISCUSSION

## 4.1 Extension of classical stiffness scaling laws

Since the majority of applications for truss lattice materials require mechanical properties only achievable by non-slender geometries, the classical scaling laws [19] fall short in predicting the stiffness response of most relevant lattice materials. Accounting for the effect of nodes as in Sec. 3.1 allows predictions to come closer to the actual material response. Starting with the theoretical framework used in the classical scalings, the effective stiffness $E^*$ scales as

$$\frac{E^*}{E_s} = C\left(\frac{r}{l}\right)^{\alpha}, \tag{4}$$

where $E_s$ is the constituent material modulus, $\alpha$ is the scaling coefficient, and $C$ is a geometric constant, applicable when $r/l \ll 1$. Given that nodes (at the same $r/l$) introduced a stiffness increase of 1-5% and 17-35% for octahedron and tetrakaidekahedron architectures as shown in

previous sections, a higher order term is necessary to account for this effect. This led to the modified scaling law

$$\frac{E^*}{E_s} = C_1 \left(\frac{r}{l}\right)^{\alpha} + C_2 \left(\frac{r}{l}\right)^{\beta}, \tag{5}$$

where $C_1$ and $C_2$ are scaling constants, and $\alpha$ and $\beta$ are scaling exponents relating to the classical theory and the nodal effects, respectively. Using dimensional analysis (details in [12]), $C_2$ can be related to the nodal geometry, such that its magnitude is directly related to the stiffening effect resulting from a specific node geometry.

Using numerical models of rigid architectures such as the octet and octahedron, and non-rigid ones like the pyramidal and tetrakaidekahedron architectures, we obtained their stiffness as a function of $r/l$, and found the parameters in Eq. 5 by fitting the model to the data. For the fitting process $\alpha$ was constrained to approximate the expected values from the classical scalings, i.e., 2 for rigid and 4 for non-rigid architectures, while $\beta$ was left unconstrained. The fits returned $\beta$ values of approximately 4 for the rigid architectures and 6 for non-rigid ones, and $C_2$ values which were directly linked to the stiffening effect of a given node geometry. For the rigid case, having exponents $\alpha = 2$ and $\beta = 4$ can be interpreted as including the contributions of stretching and bending, without assuming a dominant behavior of either. Comparison of the classical fit to the extended one in Figs. 7a,b, shows the importance of accounting for nodes particularly in the rigid case. The effect of the higher-order term is less impactful for non-rigid architectures since the behavior is bending-dominant throughout, as opposed to the rigid architectures, which transition from stretching to bending as $r/l$ increases.

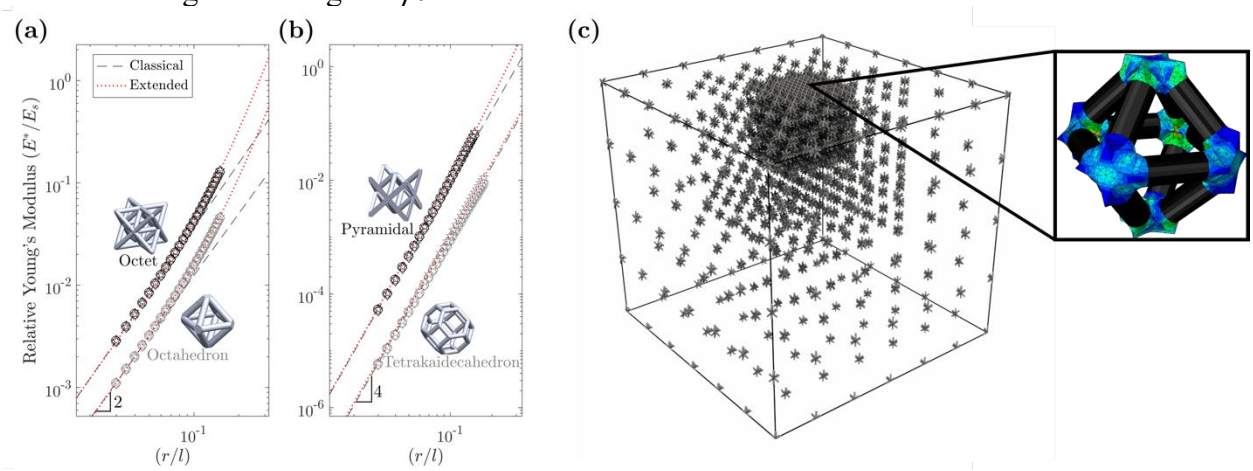



**Figure** 7. Classical and extended stiffness scaling relations fitted to numerical models of (a) rigid, and (b) non-rigid architectures; (c) diagram depicting the concept of utilizing reduced-order models for nodes within the quasicontinuum framework.

## 4.2 Interpretation of QC results

Figure 6 shows the force-displacement curves for the two fully-resolved and coarse-grained simulations. The QC simulation correctly captures the onset of buckling (seen by the drop in the force) and does a decent job matching the post-buckling response of the lattice. Furthermore, it

does this while using only a fraction of the dofs of the fully-resolved case – 3.5% of the dofs at the beginning of the simulation, and 16% of the dofs at the end of the simulation due to the refinement. This demonstrates that the QC method can be used to drastically reduce the computational size and runtime of nonlinear periodic truss lattice simulations while still retaining a high level of accuracy.

### 4.3 Towards modeling non-slender lattices with QC

We have discussed two challenges leading to computationally expensive simulations of periodic truss lattices, and techniques that can be used to remedy these issues. The higher order effects due to the non-slender nature of trusses can be addressed by using reduced order models of nodes, and the coarse-graining techniques of the QC method can be used to reduce the cost of simulations consisting of a large number of truss members.

Although not specifically addressed in the paper, it should be noted that these two techniques could be combined to model geometrically nonlinear, non-slender truss lattices using the QC method. The fully-resolved problem (Eq. 1) can be rewritten to include higher order effects from the nodes. Instead of each node containing 6 dofs (in 3D), the nodes would contain the required $6z$ dofs, where $z$ is the number of connections at the node. The unit cells would then be defined by the dofs of all of the nodes, the beams connecting nodes, and nodes themselves (Fig. 7c). The nodes can be treated as additional truss members in the unit cell energy (with a suitable weight to avoid overcounting the effect of nodes that lie in multiple unit cells), with the energy of each node being the strain energy of the reduced order models developed in Sec. 2.2. Furthermore, the linear condensed nodes could be placed in a corotational framework in order to model geometric nonlinearity in the same way linear beams were embedded in a corotational framework in [18] to model buckling of the lattice.

## 5. SUMMARY

We have shown two approaches of efficient computational modeling of non-slender truss architectures and truss tessellations with many unit cells, which enable the inexpensive simulation of non-slender lattices and lattices with many more unit cells than previously possible. Since most scalable manufacturing methods can only achieve geometries closer to the non-slender truss regime, methods to model large tessellations of these complex geometries is required. To achieve this, we outline the process in which reduced-order models for truss nodes can be implemented in a larger QC framework, thus enabling the efficient modeling of complex architectures.

## 6. REFERENCES


[1] L.R. Meza, S. Das, J.R. Greer, Strong, lightweight, and recoverable three-dimensional ceramic nanolattices, Science. 345 (2014) 1322–6. doi:10.1126/science.1255908.

[2] T. Tancogne-Dejean, A.B. Spierings, D. Mohr, Additively-manufactured metallic micro-lattice materials for high specific energy absorption under static and dynamic loading, Acta Mater. 116 (2016) 14–28. doi:https://doi.org/10.1016/j.actamat.2016.05.054.

[3] J. Bauer, A. Schroer, R. Schwaiger, O. Kraft, Approaching theoretical strength in glassy carbon nanolattices, Nat. Mater. 8 (2016). doi:10.1038/NMAT4561.

[4] L. Salari-Sharif, L. Valdevit, Accurate Stiffness Measurement of Ultralight Hollow Metallic Microlattices by Laser Vibrometry, Exp. Mech. (2014). doi:10.1007/s11340-014-9917-8.

[5] L.J. Gibson, M.F. Ashby, Cellular Solids: Structure and Properties, 2nd ed., Cambridge University Press, Cambridge, 1999.

[6] L.R. Meza, G.P. Phlipot, C.M. Portela, A. Maggi, L.C. Montemayor, A. Comella, D.M. Kochmann, J.R. Greer, Reexamining the mechanical property space of three-dimensional lattice architectures, Acta Mater. 140 (2017) 424–432. doi:https://doi.org/10.1016/j.actamat.2017.08.052.

[7] S. Pellegrino, C.R. Calladine, Matrix Analysis of Statically and Kinematically Indeternimate Frameworks, Int. J. Solids Struct. 22 (1986) 409–428.

[8] C.M. Portela, J.R. Greer, D.M. Kochmann, Impact of node geometry on the effective stiffness of non-slender three-dimensional truss lattice architectures, Extrem. Mech. Lett. (2018). doi:10.1016/j.eml.2018.06.004.

[9] L.A.A. Beex, R.H.J. Peerlings, M.G.D. Geers, A quasicontinuum methodology for multiscale analyses of discrete microstructural models, (2011) 701–718. doi:10.1002/nme.

[10] L.A.A. Beex, R.H.J. Peerlings, M.G.D. Geers, A multiscale quasicontinuum method for dissipative lattice models and discrete networks, J. Mech. Phys. Solids. 64 (2014) 154–169. doi:https://doi.org/10.1016/j.jmps.2013.11.010.

[11] L.A.A. Beex, P. Kerfriden, T. Rabczuk, S.P.A. Bordas, Quasicontinuum-based multiscale approaches for plate-like beam lattices experiencing in-plane and out-of-plane deformation, Comput. Methods Appl. Mech. Eng. 279 (2014) 348–378. doi:10.1016/j.cma.2014.06.018.

[12] O. Rokoš, R.H.J. Peerlings, J. Zeman, eXtended variational quasicontinuum methodology for lattice networks with damage and crack propagation, Comput. Methods Appl. Mech. Eng. 320 (2017) 769–792. doi:https://doi.org/10.1016/j.cma.2017.03.042.

[13] J.S. Amelang, G.N. Venturini, D.M. Kochmann, Summation rules for a fully nonlocal energy-based quasicontinuum method, J. Mech. Phys. Solids. 82 (2015) 378–413. doi:https://doi.org/10.1016/j.jmps.2015.03.007.

[14] G.P. Phlipot, D.M. Kochmann, A quasicontinuum theory for the nonlinear mechanical response of general periodic truss lattices, J. Mech. Phys. Solids J. Homepage. 124 (2018) 758–780. doi:10.1016/j.jmps.2018.11.014.

[15] L.J. Gibson, M.F. Ashby, Cellular Solids: Structure and Properties, Cambridge University Press, 1997. https://books.google.com/books?id=3wW8bwAACAAJ.